U1 small nuclear ribonucleoprotein complex and RNA splicing alterations in Alzheimer's disease

Bing Bai[a,1], Chadwick M. Hales[b,c,1], Ping-Chung Chen[a,1], Yair Gozal[b,c,1], Eric B. Dammer[c], Jason J. Fritz[b,c], Xusheng Wang[d], Qiangwei Xia[c], Duc M. Duong[c], Craig Street[e], Gloria Cantero[f,g], Dongmei Cheng[c], Drew R. Jones[a], Zhiping Wu[a], Yuxin Li[a], Ian Diner[c], Craig J. Heilman[b,c], Howard D. Rees[b,c], Hao Wu[h], Li Lin[e], Keith E. Szulwach[e], Marla Gearing[c,i], Elliott J. Mufson[j], David A. Bennett[j], Thomas J. Montine[k], Nicholas T. Seyfried[c,l], Thomas S. Wingo[b,c], Yi E. Sun[f], Peng Jin[c,e], John Hanfelt[c,h], Donna M. Willcock[m], Allan Levey[b,c,2], James J. Lah[b,c,2], and Junmin Peng[a,d,2]

[a]Departments of Structural Biology and Developmental Neurobiology and [d]St. Jude Proteomics Facility, St. Jude Children's Research Hospital, Memphis, TN 38105; Departments of [b]Neurology, [e]Human Genetics, [h]Biostatistics and Bioinformatics, [i]Pathology, and [l]Biochemistry and [c]Center for Neurodegenerative Diseases, Emory University, Atlanta, GA 30322; [f]Departments of Molecular and Medical Pharmacology and Psychiatry and Behavioral Sciences, University of California, Los Angeles, CA 91301; [g]Departmento de Fisiología Médica y Biofísica and Centro de Investigación Biomédica en Red sobre Enfermedades Neurodegenerativas, Instituto de Biomedicina de Sevilla, University Hospital Virgen del Rocío, University of Sevilla, 41013 Seville, Spain; [j]Department of Neurological Sciences, Rush University Medical Center, Chicago, IL 60612; [k]Department of Pathology, University of Washington, Seattle, WA 98104; and [m]Department of Physiology and Sanders–Brown Center on Aging, University of Kentucky, Lexington, KY 40536

Edited by Gideon Dreyfuss, University of Pennsylvania, Philadelphia, PA, and approved August 12, 2013 (received for review May 30, 2013)

Deposition of insoluble protein aggregates is a hallmark of neurodegenerative diseases. The universal presence of β-amyloid and tau in Alzheimer's disease (AD) has facilitated advancement of the amyloid cascade and tau hypotheses that have dominated AD pathogenesis research and therapeutic development. However, the underlying etiology of the disease remains to be fully elucidated. Here we report a comprehensive study of the human brain-insoluble proteome in AD by mass spectrometry. We identify 4,216 proteins, among which 36 proteins accumulate in the disease, including U1-70K and other U1 small nuclear ribonucleoprotein (U1 snRNP) spliceosome components. Similar accumulations in mild cognitive impairment cases indicate that spliceosome changes occur in early stages of AD. Multiple U1 snRNP subunits form cytoplasmic tangle-like structures in AD but not in other examined neurodegenerative disorders, including Parkinson disease and frontotemporal lobar degeneration. Comparison of RNA from AD and control brains reveals dysregulated RNA processing with accumulation of unspliced RNA species in AD, including myc box-dependent-interacting protein 1, clusterin, and presenilin-1. U1-70K knockdown or antisense oligonucleotide inhibition of U1 snRNP increases the protein level of amyloid precursor protein. Thus, our results demonstrate unique U1 snRNP pathology and implicate abnormal RNA splicing in AD pathogenesis.

proteomics | liquid chromatography-tandem mass spectrometry | U1A | RNA-seq | premature cleavage and polyadenylation

Deposition of insoluble protein aggregates is a prominent feature of neurodegenerative diseases. Identification of the aggregated proteins provides crucial insights into molecular pathogenesis, such as β-amyloid (Aβ) and tau in Alzheimer's disease (AD) (1–3), α-synuclein in Parkinson disease (PD) (4, 5), and TDP-43 in ubiquitin-positive frontotemporal lobar degeneration (FTLD-U) and amyotrophic lateral sclerosis (ALS) (6). In AD, studies of amyloid (7) and tau (8) have provided extensive knowledge concerning pathogenic mechanisms; however, the underlying etiology of the disease remains incompletely understood (9).

Unbiased approaches have great potential to shed new light on AD pathogenesis. For example, genome-wide association studies have identified a growing list of more than 10 genes linked to AD risk. Advances in proteomics technologies (10, 11) allow unparalleled opportunities to directly examine protein level differences in neurodegenerative diseases. These differences can be used to develop biomarkers of disease and provide insights into disease pathogenesis. Feasibility of a proteomics approach as well as disease-relevant changes have been described in both plasma (12–14) and cerebrospinal fluid (15–17), highlighting the utility of proteomics in biomarker development. We, and others, have also demonstrated the potential for this approach in identifying neurodegenerative-specific changes in postmortem brain tissues. Using subproteome studies, constituents of isolated amyloid plaques (18), AD hippocampus (19), cortical Lewy bodies (20), AD membrane fraction (21), and specific phosphorylation sites in neurofibrillary tangles (22) were identified. Using broader discovery proteomics, we demonstrated unique candidate proteins in both AD (23, 24) and FTLD-U (25).

To achieve more detailed characterization of abnormally aggregated proteins in AD, we undertook a comprehensive study of the human brain-insoluble proteome in AD and other neurodegenerative diseases by liquid chromatography-tandem mass spectrometry (LC-MS/MS). Among the proteins that accumulate in the AD-insoluble proteome, we identified several components of the U1 small nuclear ribonucleoprotein (U1 snRNP), which is a constituent of the spliceosome complex responsible for RNA processing. Pathological examination demonstrated striking and widespread accumulation of extranuclear aggregated U1 snRNP components in neuronal cell bodies. Functional consequences of these observations were reflected in widespread alterations in RNA processing in human AD brains. Our findings demonstrate a unique pathological association and suggest that disruption of neuronal RNA processing may play a key role in AD pathogenesis.

Results and Discussion

LC-MS/MS Analysis Reveals an Enrichment of U1 snRNP in the AD Proteome Compared with Other Neurodegenerative Proteinopathies. We designed a pooling strategy with replicates (26) to simplify the analysis of protein aggregates in cortical tissue harvested from 10 AD and 10 age-matched, nondemented cases (Fig. 1*A*; Fig. S1, and Dataset S1). Aggregated proteins typically show low

Author contributions: B.B., C.M.H., Y.G., E.B.D., A.L., J.J.L., and J.P. designed research; B.B., C.M.H., P.-C.C., Y.G., E.B.D., J.J.F., X.W., Q.X., D.M.D., C.S., G.C., D.C., Z.W., Y.L., I.D., C.J.H., H.D.R., L.L., and N.T.S. performed research; M.G., E.J.M., D.A.B., T.J.M., D.M.W., and J.P. contributed new reagents/analytic tools; B.B., C.M.H., P.-C.C., E.B.D., J.J.F., X.W., Q.X., D.M.D., C.S., D.R.J., Z.W., Y.L., H.W., L.L., K.E.S., N.T.S., T.S.W., Y.E.S., P.J., J.H., A.L., J.J.L., and J.P. analyzed data; and B.B., C.M.H., P.-C.C., A.L., J.J.L., and J.P. wrote the paper.

The authors declare no conflict of interest.

This article is a PNAS Direct Submission.

Data deposition: The sequences reported in this paper has been deposited in the ProteomeXchange database, www.proteomexchange.org (identifier PXD000067); and raw RNA-seq files have been deposited in the National Center for Biotechnology Information Sequence Read Archive database, www.ncbi.nlm.nih.gov/sra (accession no. SRA060572).

[1]B.B., C.M.H., P.-C.C., and Y.G. contributed equally to this work.

[2]To whom correspondence may be addressed. E-mail: junmin.peng@stjude.org, jlah@emory.edu, or alevey@emory.edu.

This article contains supporting information online at www.pnas.org/lookup/suppl/doi:10.1073/pnas.1310249110/-/DCSupplemental.

Downloaded at Palestinian Territory, occupied on December 1, 2021

www.manaraa.com

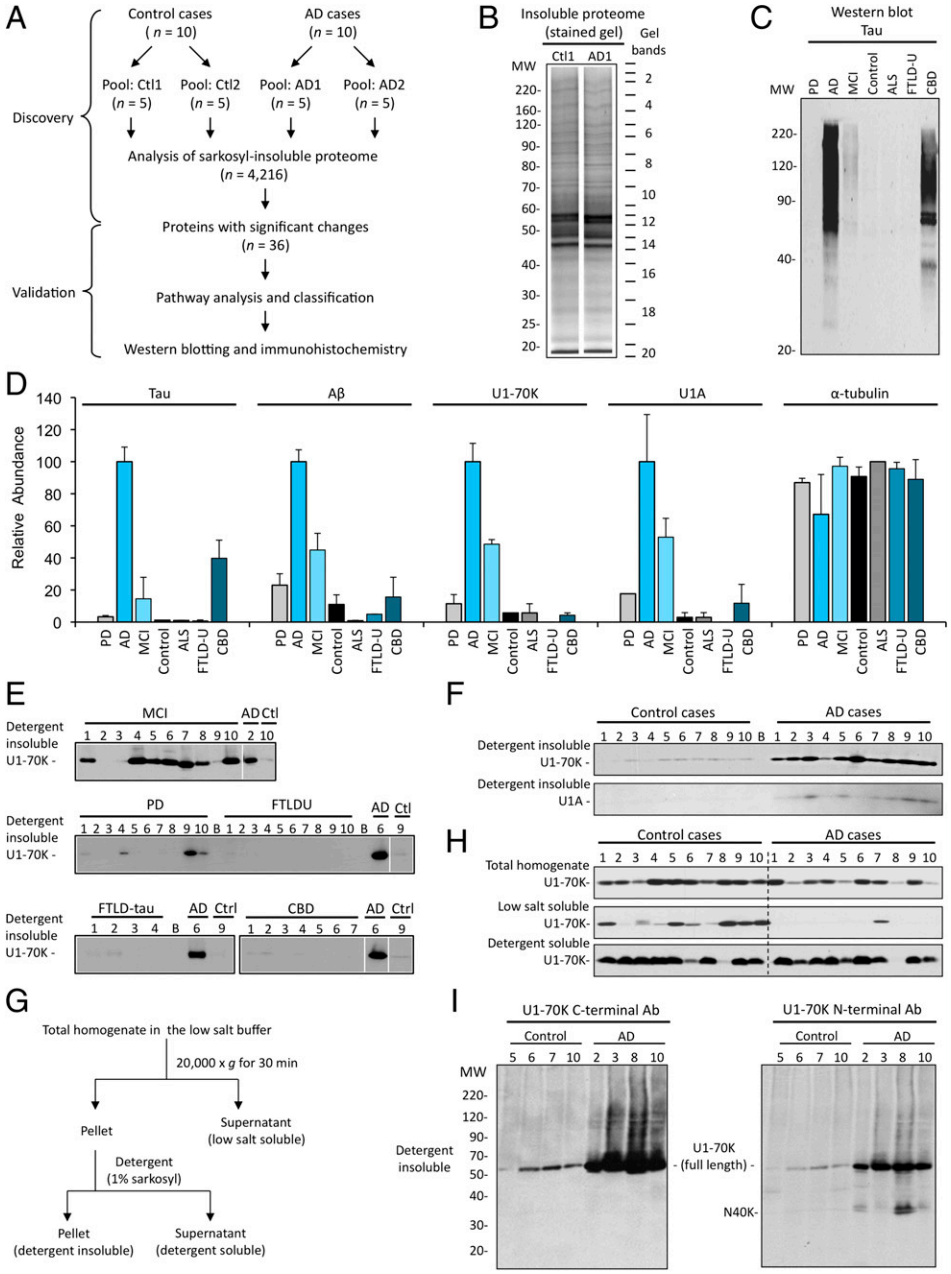

Fig. 1. Proteomic comparison reveals that U1-70K and U1A are enriched in the sarkosyl-insoluble proteome of AD. (*A*) Scheme for profiling the aggregated proteins in AD postmortem brains, with nondemented cases as controls (Ctl). (*B*) A stained SDS gel showing detergent-insoluble proteins in one set of pooled control and AD cases. (*C*) Similar proteomics analysis of seven groups of neurodegenerative disease samples. One set of sarkosyl-insoluble fractions was immunoblotted by phosphorylated tau antibodies to confirm tauopathies. (*D*) Relative level of representative sarkosyl-insoluble proteins across different diseases. The level was estimated by spectral counts of these identified proteins, and normalized to set the maximum to 100. Two replicates were analyzed, and the bars indicate the values of mean ± SEM. (*E–I*) Western blotting analysis of U1-70K or U1A in biochemical brain extracts from control and neurodegenerative cases, and the strategy for protein sequential extraction. The case numbers are shown. B, blank. The exposure time was longer in *I Left* than in others. At least one AD sample and one control sample were loaded on every gel for comparison.

solubility and differential extraction with the anionic detergent sarkosyl has been commonly used to enrich for aggregated tau (27), α-synuclein (28), and TDP-43 (6). We thus prepared and analyzed sarkosyl-insoluble fractions by gel electrophoresis (Fig. 1*B*) and LC-MS/MS. A total of 4,216 proteins were identified (<1% false discovery rate; raw data has been deposited at www.proteomexchange.org, identifier PXD000067), and 36 proteins accumulated in AD (<5% false discovery rate by two statistical approaches; Table 1). As expected, Aβ and tau were abundantly enriched in AD, together with other known proteins regulating Aβ metabolism (29). Consistent with the notion that inflammation (30), phosphorylation networks (8), synaptic plasticity (31), and mitochondrial regulation (32) are altered in AD, we found that numerous proteins involved in these pathways are preferentially enriched in the disease tissues. Interestingly, we observed that two subunits (U1-70K and U1A) of the U1 snRNP and the associated RNA helicase Prp5 (33) were highly elevated in the AD-insoluble proteome, indicating possible deposition of the U1 snRNP.

We used the same proteomics strategy to analyze cases of PD, FTLD-U, ALS, and corticobasal degeneration (CBD; Dataset S1), and determined whether the U1 snRNP changes are specific to AD or common in other diseases with protein aggregates. We also studied cases of mild cognitive impairment (MCI), which is often a prodromal stage of AD, to determine if proteomic changes occur early in the disease. As anticipated, the level of detergent insoluble tau was high in AD and CBD (a prototypical tauopathy), lower in MCI, and barely detectable in PD, FTLD-U, and ALS (Fig. 1 *C* and *D*); Aβ also showed a marked increase in AD, a moderate increase in MCI, but no accumulation in the other diseases. Importantly, the levels of insoluble U1-70K and U1A were highly correlated with that of Aβ rather than tau, supporting the conclusion that U1 snRNP accumulation is specific to AD and occurs early during the disease development.

To confirm the proteomic changes and further analyze the aggregation of U1 snRNP proteins in individual cases, we used specific antibodies (Fig. S2) to probe for U1-70K and U1A in brain extracts (Fig. 1 *E* and *F*). The detergent insoluble U1-70K

MEDICAL SCIENCES
Downloaded at Palestinian Territory, occupied on December 1, 2021
www.manaraa.com

Table 1. Identified proteins that are accumulated in AD vs. control cases

Accession no.	Protein names	Spectral counts* Ctl1	Ctl2	AD1	AD2
Aβ peptide metabolism					
NP_000475.1	Aβ peptide	9	31	169	196
NP_000032.1	Apolipoprotein E	1	1	49	92
NP_115907.2	Collagen, type XXV, alpha 1 isoform 2	1	0	23	24
NP_004369.1	Cellular retinoic acid binding protein 1	0	0	9	7
Cytoskeleton maintenance					
NP_058519.2	Microtubule-associated protein tau	10	11	824	989
NP_116757.2	Dystrobrevin alpha	0	11	23	24
Inflammation					
NP_009224.2	Complement component 4a preproprotein	7	7	77	128
NP_001002029.3	Complement component 4b preproprotein	7	7	81	163
NP_000055.2	Complement component 3	1	2	57	93
Protein phosphorylation					
NP_005246.2	Cyclin G-associated kinase	0	1	7	11
NP_002842.2	Protein tyrosine phosphatase, zeta1	2	0	9	10
NP_644812.1	T-cell activation protein phosphatase 2C	0	0	6	7
Synaptic plasticity					
NP_982271.1	Synaptojanin 1	17	9	59	56
NP_001626.1	Amphiphysin	16	14	44	35
NP_640337.3	Syntaxin binding protein 5	2	9	24	22
NP_055804.2	Regulating synaptic membrane exocytosis 1	0	2	12	11
NP_056993.2	Neuroblastoma-amplified protein (with a Sec39 domain)	0	0	4	10
NP_066973.1	Glutamate receptor interacting protein 1	0	0	7	7
Mitochondrial regulation					
NP_892022.2	Mitochondrial nicotinamide nucleotide transhydrogenase	46	46	133	95
NP_066923.3	Mitochondrial NFS1 nitrogen fixation 1	11	17	45	40
NP_000134.2	Mitochondrial fumarate hydratase	5	12	34	33
NP_570847.1	Optic atrophy 1	1	2	15	15
NP_004270.2	Mitochondrial processing peptidase	1	1	13	8
RNA splicing					
NP_003080.2	U1 small nuclear ribonucleoprotein 70 kDa	2	2	31	39
NP_004587.1	U1 small nuclear ribonucleoprotein A	0	1	12	22
NP_055644.2	ATP-dependent RNA helicase DDX46, Prp5	0	0	9	17
Metabolic reactions					
NP_001120920.1	4-Aminobutyrate aminotransferase	20	25	56	60
NP_036322.2	10-Formyltetrahydrofolate dehydrogenase	10	16	40	33
NP_001094346.1	Phytanoyl-CoA dioxygenase domain containing protein 1	0	0	9	7
NP_835471.1	Nicotinamide nucleotide adenylyltransferase 3	0	0	7	4
NP_149078.1	Asparagine-linked glycosylation 2	0	0	5	4
Others					
NP_056450.2	GTPase activating protein and VPS9 domains 1	1	2	13	13
NP_065871.2	Phosphatidylinositol-dependent Rac exchanger 1 (P-REX1)	0	0	5	6
NP_006086.1	Aminophospholipid transporter	9	6	24	29
NP_055839.3	RAN binding protein 16 (exportin 7)	3	8	24	24
NP_055806.2	ALFY, involved in macroautophagy	0	0	5	4

Results of two control case pools (Ctl1 and Ctl2) and two AD case pools (AD1 and AD2). These proteins elevated in AD were analyzed by two statistical approaches (false discovery rate <5%) with accession no. in National Center for Biotechnology Information Reference Sequence Database. Aβ, ApoE, tau, and RNA splicing factors are shaded.
*Spectral counts are used as a quantitative index.

was increased in all 10 AD cases as well as in 7 of 10 MCI cases; U1A accumulated in 8 of 10 AD cases. In contrast, U1-70K was not aggregated in any other cases of PD, FTLD-U, FTLD-tau, and CBD, except in three PD samples. Reexamination of these three PD cases with additional histochemical staining identified coexisting AD plaque and tangle pathology. These data strongly validate the uniqueness of U1 snRNP accumulation to AD.

Biochemical Confirmation of U1 snRNP Alterations in AD. We next sought to examine the total protein level of U1-70K and to characterize U1-70K biochemically in the AD brain. Samples were homogenized and extracted using three buffers with increasing stringency: a low-salt buffer, a sarkosyl-containing solution, and 8 M urea (Fig. 1*G*). In a comparison of AD and control cases (Fig. 1*H*), U1-70K displayed no obvious difference

Downloaded at Palestinian Territory, occupied on December 1, 2021
www.manaraa.com

in either the total homogenate or the sarkosyl soluble fraction. Intriguingly, the low salt-extracted U1-70K was decreased in AD cases (~threefold difference; $P < 0.01$; Fig. S3). This result, together with the enrichment of U1-70K in the sarkosyl-insoluble (i.e., urea) samples, indicates that the biophysical characteristics of U1-70K are altered in AD, resulting in its aggregation and depletion from the low salt-soluble pool. These findings suggest a possible loss of U1-70K function in AD.

Aggregation of protein fragments is common in neurodegeneration (34, 35). We found that in the AD samples, U1-70K was identified by mass spectrometry in two regions of the SDS gels (~70 kDa and ~40 kDa; Fig. 1*B*), and the 40-kDa region contained only N-terminal peptides of U1-70K. The heterogeneous N-terminal fragments were confirmed by immunoblotting using antibodies specific to either N terminus or C terminus of U1-70K (Fig. 1*I*). Thus, U1-70K is internally cleaved and the resulting N-terminal fragments are detected in the detergent-insoluble proteome. We examined U1-70K for characteristics of prion-like domains (PrLDs) that were recently identified in heterogeneous nuclear ribonucleoproteins (hnRNP) in multisystem proteinopathy and ALS (36). Though structural analysis (37) indicates that the first 100-residue region in U1-70K is intrinsically disordered and may contribute to the aggregation process, no PrLDs were identified.

U1 snRNP Forms Tangle-Like Inclusions in AD Brain. Immunohistochemical analysis was performed to examine the localization and accumulation of U1 snRNP components in AD. These studies revealed that U1-70K and U1A form cytoplasmic tangle-like aggregates in 17/20 and 9/10 AD cases, respectively, but not in controls (Fig. 2 *A–D*; Dataset S1). These pathological changes were not present in FTLD-U and FTLD-tau cases (Fig. 2 *E–H*) despite the presence of TDP-43 (Fig. 2*F*) and tau (Fig. 2*H*) pathology. PD and CBD cases also did not show abnormal accumulations of U1 snRNP protein components (Dataset S1). Antibodies against the 2,2,7-trimethylguanosine cap that is characteristic of spliceosomal RNAs also stained cytoplasmic tangle-like aggregates (Fig. S4 *M* and *N*), and quantitative RT-PCR showed enrichment of U1 snRNA in the AD-insoluble fraction (Fig. S5*A*). Other RNA splicing factors, such as hnRNP A/B, recently suggested as a dysfunctional splicing factor in AD (38), and serine/arginine repetitive matrix protein 2 (SRRM2), did not demonstrate tangle-like aggregates, suggesting that this may be a U1 snRNP-specific process (Fig. S4 *A–D*). Although pure tauopathies (e.g., FTLD-tau and CBD) do not show U1-70K aggregation, double staining of AD cases indicates that U1-70K inclusions are closely associated with tau-immunoreactive neurofibrillary tangles (NFTs; Fig. 2 *I–L*), implying possible relationship between the mechanisms of U1-70K and tau deposition in AD. To better define the relationship of U1-70K pathology to that of NFTs, we examined hippocampus and temporal, frontal, and occipital cortices of AD cases with progressively severe neurofibrillary pathology (Braak stages 0, III, and VI). The appearance of U1-70K spreads across the brain in a sequence similar to that seen for tau NFTs (Fig. S4*O*). Dramatic progression in U1-70K pathology between Braak stage III and VI leads to uniform accumulation in all brain regions (Fig. S4 *E–L*). These data are highly consistent with our biochemical analyses, strongly demonstrating specific U1 snRNP pathology in AD.

Deep RNA Sequencing Demonstrates Splicing Abnormalities in AD. The biochemical and pathological changes in U1 snRNP components in AD brains suggest a possible loss of nuclear spliceosome activity. Though alternative splicing of specific genes has been previously reported (39), global disruption of RNA processing has never been suggested in AD. To address this possibility, we performed deep RNA sequencing (40) of frontal cortex RNAs using two independent sample groups from the brain banks of Emory University (four control and five AD cases) and the University of Kentucky (UKY; three control and three AD cases). In both groups, a higher proportion of AD brain-derived reads mapped to intronic sequences of known genes ($P = 0.041$ in Emory cases, $P = 0.003$ in UKY cases; Fig. 3*A*). For individual genes, we further defined the ratio between length-normalized intronic and exonic reads as a splicing deficiency score. The distribution of the splicing deficiency scores of all mapped genes clearly indicated splicing defects in AD ($n = 10{,}490$ in Emory group, $n = 14{,}583$ in UKY group; $P < 2.2 \times 10^{-16}$ in both groups; Fig. 3*B*). A large number of genes were affected in AD (3,014 genes with high splicing deficiency scores in both Emory and UKY AD cases, 5% false discovery rate, by two statistical approaches; Fig. 3*B* and Dataset S2). To confirm these findings, we applied the NanoString approach (41) to analyze 12 selected transcripts implicated in AD pathogenesis using high-quality RNA samples (average RNA integrity number score = 8.0; 14 control and 15 AD cases; Dataset S1). For each gene, we quantified the ratio

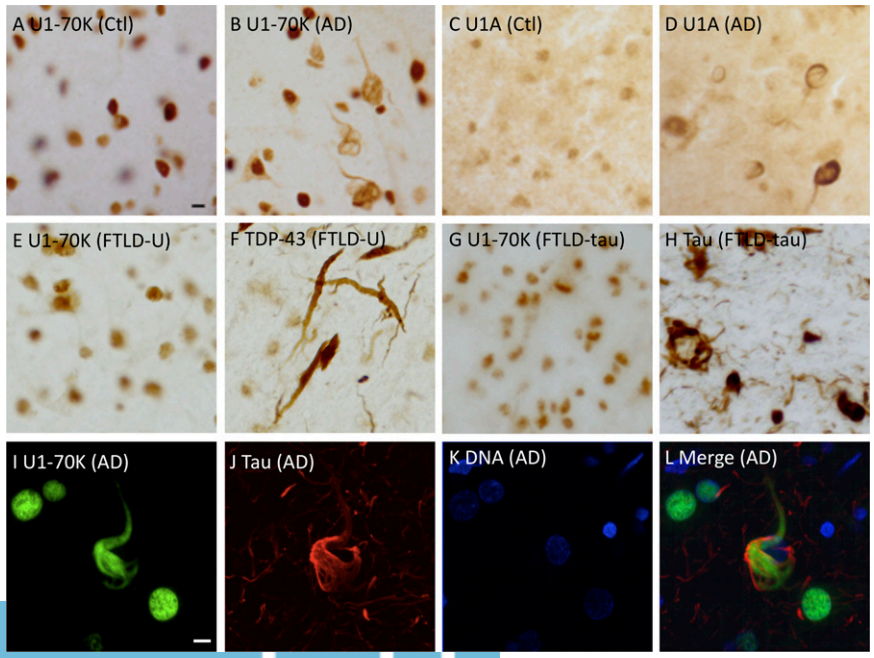

Fig. 2. U1-70K and U1A show neurofibrillary tangles in AD pathology. (*A–D*) Representative immunohistochemistry images with diaminobenzidine staining of selected control and AD brain slides (50-μm sections). (Scale bar, 5 μm.) (*E–H*) Representative adjacent sections of FTLD-U and FTLD-tau cases demonstrating normal U1-70K distribution despite the presence of TDP-43 and tau pathology, respectively. (*I–L*) Double-immunofluorescence staining indicates partial colocalization of U1-70K with tau in AD. (Scale bar, 5 μm.)

Downloaded at Palestinian Territory, occupied on December 1, 2021
www.manaraa.com

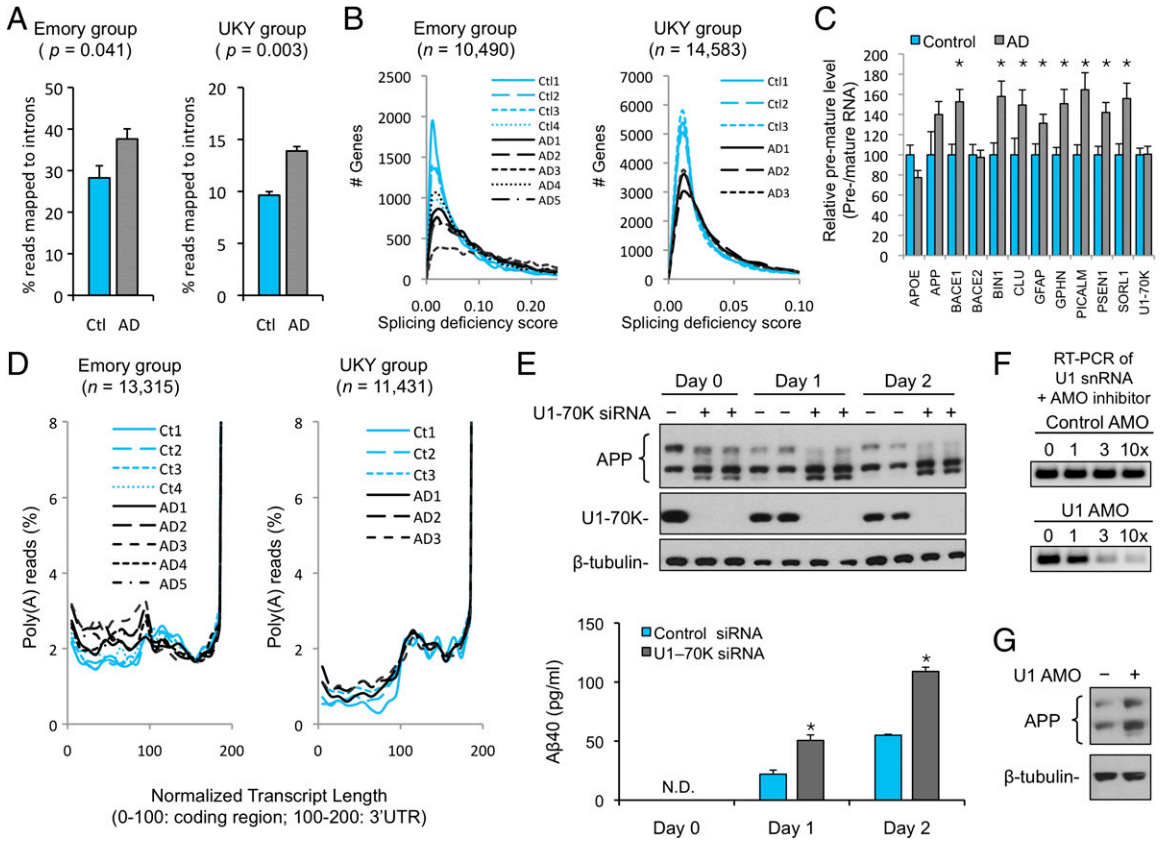

Fig. 3. RNA splicing impairment in AD, and APP up-regulation upon splicing inhibition. (*A*) The frequency of summed intron reads is higher in AD than in control. The bars indicate mean ± SEM (*P* value derived by Student *t* test). The Emory and UKY samples were processed independently. The batch discrepancy may be due to sample quality difference and experimental variations. (*B*) The histograms of splicing deficiency scores of all mapped genes show a statistically significant difference between AD and control in both Emory and UKY groups ($P < 2.2 \times 10^{-16}$ for both groups, Kolmogorov–Smirnov test). (*C*) Evaluation of RNA splicing efficiency by measuring mRNAs and pre-mRNAs of selected genes in control and AD cases. The bars indicate the values of mean ± SEM (AD: $n = 15$; control: $n = 14$; asterisks: $P < 0.05$, Student *t* test). (*D*) Poly(A)-containing reads from 5′ to 3′ of every gene were defined and normalized according to the total poly(A) reads of the gene. Every transcript was divided into coding region (0–100, from start to stop codon) and 3′ UTR region (100–200), then into 20 bins. The poly(A) read percentage in each bin was averaged for all genes in every case, and plotted to represent the frequency of PCPA. The PCPA frequency was markedly different between control and AD cases ($P < 2.2 \times 10^{-16}$ for Emory group, $P < 6.9 \times 10^{-15}$ for UKY group, Kolmogorov–Smirnov test). (*E*) U1-70K knockdown increases APP and Aβ40 levels in HEK293 cells. The cells were transfected for 2 d, then cultured in a low-serum medium and harvested at day 0, 1, and 2 for analysis (asterisks: $P < 0.05$, Student *t* test; N.D., not detected). APP and Aβ40 were analyzed by immunoblotting and ELISA, respectively. (*F*) PCR to examine the specificity of U1 AMO. The reaction was designed to amplify the U1 RNA 5′-end region with the addition of control AMO or U1 AMO as inhibitory competitor. (*G*) The APP level increases upon AMO inhibition of U1 snRNP.

between pre-mRNAs and mature mRNAs, comparing abundance of exon1–intron1 junction sequences to exon1–exon2 junction sequences, as a measure of splicing efficiency. The splicing efficiency for eight transcripts in the AD cases showed significant reduction (i.e., a relative increase in intron 1-containing RNAs; $P < 0.05$; Fig. 3*C* and Dataset S3). Finally, using traditional quantitative RT-PCR methods, we validated the results for three transcripts genetically linked to AD pathogenesis: myc box-dependent-interacting protein 1, clusterin, and presenilin-1 (Fig. S5*B*). Taken together, these results strongly support a profound alteration in RNA processing in AD.

In addition to a role in splicing, U1 snRNP is recruited to nascent transcripts to suppress premature cleavage and polyadenylation (PCPA) on cryptic poly(A) sites, and moderate inhibition of U1 snRNP by antisense morpholino oligonucleotide (AMO) leads to PCPA in a 5′–3′ direction (42). We did not perform high-throughput sequencing of differentially expressed transcripts (43) in our experiments and did not have sufficient data to fully assess potential changes in telescripting in AD; however, examination of RNA sequencing (RNA-seq) data revealed more poly(A)-containing reads in the 5′ end of transcripts among AD cases than controls in both Emory and UKY groups ($n = 13{,}315$ in Emory group, $n = 11{,}431$ in UKY group; $P < 1 \times 10^{-14}$ in both groups; Fig. 3*D*). These data suggest the intriguing possibility that partial loss of U1 snRNP function in AD might result in increased PCPA in addition to altered splicing.

U1 snRNP Deficiency Alters Amyloid Precursor Protein (APP) Expression and Aβ Levels. To assess U1 snRNP loss of function in an experimental system, we performed U1-70K knockdown in HEK293 cells and sought to determine possible effects on APP metabolism. U1-70K knockdown (<10% remaining) induced an increase in endogenous APP and Aβ40 compared with the scrambled siRNA control (Fig. 3*E* and Fig. S6*A*). Human APP has three isoforms (APP_{770}, APP_{751}, and APP_{695}) generated by alternative splicing (44). RT-PCR analysis indicated that U1-70K knockdown resulted in a decrease of APP_{770} transcript and an increase of APP_{751} and APP_{695} transcripts (Fig. S6*B*). This up-regulation of APP and Aβ40 was also observed in differentiated SH-SY5Y neuroblastoma cells (Fig. S6 *C–E*). In addition to U1-70K knockdown, U1 AMO inhibition of U1 snRNP function elevated APP level as well (Fig. 3 *F* and *G*). Though we did not observe an obvious isoform-switching phenomenon in human brain, NanoString experiments found an increase in RNA species containing contiguous exon1–intron1 sequences for APP in AD ($P = 0.068$; Fig. 3*C*).

Downloaded at Palestinian Territory, occupied on December 1, 2021
www.manaraa.com

These results indicate that disruption of RNA splicing function may result in mechanistically relevant changes in APP expression.

We have discovered U1 snRNP proteinopathy and global RNA processing defects in the AD brain, and a role for U1-70K in APP metabolism. The dysregulation of core RNA splicing machinery in AD was unexpected; remarkably, it is highly disease-specific, occurs early, and is widespread in AD cases. The malfunction of these core splicing factors provides important insight into molecular mechanisms outside of Aβ and tau that contribute to AD.

Methods

Case Materials. Human postmortem frozen and paraformaldehyde-fixed tissues from cortical areas were provided from clinically and pathologically well-characterized cases at the Alzheimer's Disease Research Center (ADRC) Brain Bank at Emory University, Rush Alzheimer's Disease Center's Religious Orders Study at Rush University Medical Center, the University of Washington ADRC, and the University of Kentucky ADRC, with signed informed consents for the studies (Dataset S1). Diagnoses were made in accordance with established criteria and guidelines of control and AD (45, 46), MCI (47, 48), PD (49), FTLD-tau (50, 51), FTLD-U (50, 51), ALS (52), and CBD (53, 54). Details of proteomic and RNA-seq analyses, Western blot, immunohistochemical staining, RT-PCR, U1-70K knockdown, and U1 snRNP inhibition procedures are described in SI Methods.

ACKNOWLEDGMENTS. The authors thank P. Xu, C. H. Na, W. Tang, and R. Qi for laboratory assistance; and X. Lin, Y. Feng, D. Pallas, Z. Mao, J. Glass, S. Li, and J. P. Taylor for helpful discussion. This work was partially supported by National Institutes of Health (NIH) Grants P50AG025688, P30NS055077, and P50AG005136; Consortium for Frontotemporal Dementia Research NIH Training Grants F30NS057902 (to Y.G.), F32AG038259 (to E.B.D.), and F32NS007480 (to N.T.S.); a American Academy of Neurology Foundation Clinical Research Training Fellowship (to C.M.H.); Sara Borrell Program Support (Spanish Instituto de Salud Carlos III) (G.C.); and Grants P01GM081621 and R01MH082068 (to Y.E.S.), P01AG14449 (to E.J.M.), and P30AG10161 (to D.A.B.). J.P. is supported by the American Lebanese Syrian Associated Charities.

1. Glenner GG, Wong CW (1984) Alzheimer's disease: Initial report of the purification and characterization of a novel cerebrovascular amyloid protein. *Biochem Biophys Res Commun* 120(3):885–890.
2. Masters CL, et al. (1985) Amyloid plaque core protein in Alzheimer disease and Down syndrome. *Proc Natl Acad Sci USA* 82(12):4245–4249.
3. Lee VM, Balin BJ, Otvos L, Jr., Trojanowski JQ (1991) A68: A major subunit of paired helical filaments and derivatized forms of normal Tau. *Science* 251(4994):675–678.
4. Spillantini MG, et al. (1997) Alpha-synuclein in Lewy bodies. *Nature* 388(6645): 839–840.
5. Polymeropoulos MH, et al. (1997) Mutation in the alpha-synuclein gene identified in families with Parkinson's disease. *Science* 276(5321):2045–2047.
6. Neumann M, et al. (2006) Ubiquitinated TDP-43 in frontotemporal lobar degeneration and amyotrophic lateral sclerosis. *Science* 314(5796):130–133.
7. Hardy J, Selkoe DJ (2002) The amyloid hypothesis of Alzheimer's disease: Progress and problems on the road to therapeutics. *Science* 297(5580):353–356.
8. Ballatore C, Lee VM, Trojanowski JQ (2007) Tau-mediated neurodegeneration in Alzheimer's disease and related disorders. *Nat Rev Neurosci* 8(9):663–672.
9. Pimplikar SW, Nixon RA, Robakis NK, Shen J, Tsai LH (2010) Amyloid-independent mechanisms in Alzheimer's disease pathogenesis. *J Neurosci* 30(45):14946–14954.
10. Gstaiger M, Aebersold R (2009) Applying mass spectrometry-based proteomics to genetics, genomics and network biology. *Nat Rev Genet* 10(9):617–627.
11. Choudhary C, Mann M (2010) Decoding signalling networks by mass spectrometry-based proteomics. *Nat Rev Mol Cell Biol* 11(6):427–439.
12. Hye A, et al. (2006) Proteome-based plasma biomarkers for Alzheimer's disease. *Brain* 129(Pt 11):3042–3050.
13. German DC, et al. (2007) Serum biomarkers for Alzheimer's disease: Proteomic discovery. *Biomed Pharmacother* 61(7):383–389.
14. Wada-Isoe K, et al. (2007) Serum proteomic profiling of dementia with Lewy bodies: Diagnostic potential of SELDI-TOF MS analysis. *J Neural Transm* 114(12):1579–1583.
15. Ryberg H, et al. (2010) Discovery and verification of amyotrophic lateral sclerosis biomarkers by proteomics. *Muscle Nerve* 42(1):104–111.
16. Wijte D, et al. (2012) A novel peptidomics approach to detect markers of Alzheimer's disease in cerebrospinal fluid. *Methods* 56(4):500–507.
17. Ringman JM, et al. (2012) Proteomic changes in cerebrospinal fluid of presymptomatic and affected persons carrying familial Alzheimer disease mutations. *Arch Neurol* 69(1):96–104.
18. Liao L, et al. (2004) Proteomic characterization of postmortem amyloid plaques isolated by laser capture microdissection. *J Biol Chem* 279(35):37061–37068.
19. Sultana R, et al. (2007) Proteomics analysis of the Alzheimer's disease hippocampal proteome. *J Alzheimers Dis* 11(2):153–164.
20. Xia Q, et al. (2008) Proteomic identification of novel proteins associated with Lewy bodies. *Front Biosci* 13:3850–3856.
21. Donovan LE, et al. (2012) Analysis of a membrane-enriched proteome from postmortem human brain tissue in Alzheimer's disease. *Proteomics Clin Appl* 6(3-4):201–211.
22. Rudrabhatla P, Jaffe H, Pant HC (2011) Direct evidence of phosphorylated neuronal intermediate filament proteins in neurofibrillary tangles (NFTs): Phosphoproteomics of Alzheimer's NFTs. *FASEB J* 25(11):3896–3905.
23. Xia Q, et al. (2008) Phosphoproteomic analysis of human brain by calcium phosphate precipitation and mass spectrometry. *J Proteome Res* 7(7):2845–2851.
24. Gozal YM, et al. (2009) Proteomics analysis reveals novel components in the detergent-insoluble subproteome in Alzheimer's disease. *J Proteome Res* 8(11):5069–5079.
25. Gozal YM, et al. (2011) Proteomic analysis of hippocampal dentate granule cells in frontotemporal lobar degeneration: Application of laser capture technology. *Front Neurol* 2:24.
26. Zhou JY, Hanfelt J, Peng J (2007) Clinical proteomics in neurodegenerative diseases. *Proteomics Clin Appl* 1(11):1342–1350.
27. Spillantini MG, et al. (1997) Familial multiple system tauopathy with presenile dementia: A disease with abundant neuronal and glial tau filaments. *Proc Natl Acad Sci USA* 94(8):4113–4118.
28. Fujiwara H, et al. (2002) Alpha-synuclein is phosphorylated in synucleinopathy lesions. *Nat Cell Biol* 4(2):160–164.
29. Weiner HL, Frenkel D (2006) Immunology and immunotherapy of Alzheimer's disease. *Nat Rev Immunol* 6(5):404–416.
30. Wyss-Coray T (2006) Inflammation in Alzheimer disease: Driving force, bystander or beneficial response? *Nat Med* 12(9):1005–1015.
31. Selkoe DJ (2002) Alzheimer's disease is a synaptic failure. *Science* 298(5594):789–791.
32. Lin MT, Beal MF (2006) Mitochondrial dysfunction and oxidative stress in neurodegenerative diseases. *Nature* 443(7113):787–795.
33. Staley JP, Guthrie C (1998) Mechanical devices of the spliceosome: Motors, clocks, springs, and things. *Cell* 92(3):315–326.
34. Taylor JP, Hardy J, Fischbeck KH (2002) Toxic proteins in neurodegenerative disease. *Science* 296(5575):1991–1995.
35. Ross CA, Poirier MA (2004) Protein aggregation and neurodegenerative disease. *Nat Med* 10(Suppl):S10–S17.
36. Kim HJ, et al. (2013) Mutations in prion-like domains in hnRNPA2B1 and hnRNPA1 cause multisystem proteinopathy and ALS. *Nature* 495(7442):467–473.
37. Pomeranz Krummel DA, Oubridge C, Leung AK, Li J, Nagai K (2009) Crystal structure of human spliceosomal U1 snRNP at 5.5 A resolution. *Nature* 458(7237):475–480.
38. Berson A, et al. (2012) Cholinergic-associated loss of hnRNP-A/B in Alzheimer's disease impairs cortical splicing and cognitive function in mice. *EMBO Mol Med* 4(8):730–742.
39. Mills JD, Janitz M (2012) Alternative splicing of mRNA in the molecular pathology of neurodegenerative diseases. *Neurobiol Aging* 33(5):1012.e1011–1024.
40. Mortazavi A, Williams BA, McCue K, Schaeffer L, Wold B (2008) Mapping and quantifying mammalian transcriptomes by RNA-Seq. *Nat Methods* 5(7):621–628.
41. Geiss GK, et al. (2008) Direct multiplexed measurement of gene expression with color-coded probe pairs. *Nat Biotechnol* 26(3):317–325.
42. Kaida D, et al. (2010) U1 snRNP protects pre-mRNAs from premature cleavage and polyadenylation. *Nature* 468(7324):664–668.
43. Berg MG, et al. (2012) U1 snRNP determines mRNA length and regulates isoform expression. *Cell* 150(1):53–64.
44. Rockenstein EM, et al. (1995) Levels and alternative splicing of amyloid β protein precursor (APP) transcripts in brains of APP transgenic mice and humans with Alzheimer's disease. *J Biol Chem* 270(47):28257–28267.
45. Mirra SS, et al. (1991) The Consortium to Establish a Registry for Alzheimer's Disease (CERAD). Part II. Standardization of the neuropathologic assessment of Alzheimer's disease. *Neurology* 41(4):479–486.
46. Hyman BT, Trojanowski JQ (1997) Consensus recommendations for the postmortem diagnosis of Alzheimer disease from the National Institute on Aging and the Reagan Institute Working Group on diagnostic criteria for the neuropathological assessment of Alzheimer disease. *J Neuropathol Exp Neurol* 56(10):1095–1097.
47. Petersen RC, et al. (1999) Mild cognitive impairment: Clinical characterization and outcome. *Arch Neurol* 56(3):303–308.
48. Ritchie K, Artero S, Touchon J (2001) Classification criteria for mild cognitive impairment: A population-based validation study. *Neurology* 56(1):37–42.
49. Gelb DJ, Oliver E, Gilman S (1999) Diagnostic criteria for Parkinson disease. *Arch Neurol* 56(1):33–39.
50. Trojanowski JQ, Dickson D (2001) Update on the neuropathological diagnosis of frontotemporal dementias. *J Neuropathol Exp Neurol* 60(12):1123–1126.
51. McKhann GM, et al.; Work Group on Frontotemporal Dementia and Pick's Disease (2001) Clinical and pathological diagnosis of frontotemporal dementia: Report of the Work Group on Frontotemporal Dementia and Pick's Disease. *Arch Neurol* 58(11): 1803–1809.
52. Ince PG, Lowe J, Shaw PJ (1998) Amyotrophic lateral sclerosis: Current issues in classification, pathogenesis and molecular pathology. *Neuropathol Appl Neurobiol* 24(2): 104–117.
53. Dickson DW, et al.; Office of Rare Diseases of the National Institutes of Health (2002) Office of Rare Diseases neuropathologic criteria for corticobasal degeneration. *J Neuropathol Exp Neurol* 61(11):935–946.
54. Dickson DW (2001) Neuropathology of Pick's disease. *Neurology* 56(11, Suppl 4): S16–S20.

Downloaded at Palestinian Territory, occupied on December 1, 2021

www.manaraa.com